Pulsed electric field applied to biological tissue: measurement set-up to evaluate electrical resistivity

M Bullo, F Dughiero, M Forzan, E Sieni

Pulsed electric field applied to biological tissue: measurement set-up to evaluate electrical resistivity

M. Bullo[1a], F. Dughiero[1b], M. Forzan[1c] and E. Sieni[1d]

[1]University of Padova, Department of Industrial Engineering, via Gradenigo 6/A, 35131 Padova, Italy

Corresponding author: michele.forzan@unipd.it

Abstract
In this paper we present the design of a measurement set-up to evaluate electrical resistivity of biological tissues.

Key words: electrical resistivity, biological tissues, measurement set-up, electroporation.

Introduction

Electrochemotherapy (ECT) uses voltage pulses (e.g. 8 rectangular pulses at 1000V @ 5 kHz) applied to a biological tissue by means of pairs of implanted needles. Electroporation modifies cell membrane permeation to genes or drugs by opening transmembrane pores [1], [2]. This technique is currently exploited in medicine to treat some cutaneous and subcutaneous tumors, e.g. melanoma, soft tissue sarcomas, etc. [2]–[5]. In fact cell, membrane modifications due to the application of an electric field can improve the uptake of low permeate chemotherapeutic drugs in cancer cells.
Electrical properties of tissues depend on cell size and density [6]–[8]. In recent literature the electrical resistivity of electroporated tissue has been modeled as a non-linear equation on electric field intensity [9]:

$$\rho^{-1}(\|\boldsymbol{E}\|) = \rho_0^{-1} + \frac{\rho_1^{-1} + \rho_0^{-1}}{2}\left[1 + \tanh(k(\|\boldsymbol{E}\| - E_{th}))\right] \tag{1}$$

where ρ_0 and ρ_1 are the resistivity values before and after electroporation, E_{th} the electric field threshold and k a fitting coefficient [9]. The threshold of electric field, E_{th} that induces cell electroporation depends on the tissue type [10].
In this contribution a measurement set-up, designed to evaluate the tissue resistivity is investigated. This study is relevant in order to evaluate the electrical properties of different type of tumor. This information can be used to tune the clinical technique for different tumors that are currently treated by ECT (e.g. melanoma).

The method

The measurements of resistance have been done by the classical four point method [11], [12]. The same method has been used also by other authors in order to characterize the biological tissue resistivity [13]–[15]. Considering Fig. 1 where four electrodes are implanted at a distance d in the material to characterize. The two external electrodes, implanted at a depth L, are supplied by an electrical current, whereas the two internal electrodes are connected to a voltmeter to evaluate the voltage difference. The optimal value of L has been determined by numerical computations. Given the electrodes distance, d, and the voltage, V_m, and current, I_m, the measured resistivity is given by:

$$\rho = \frac{V_m}{I_m} 2\pi d \tag{2}$$

The first sensor has been realized by modifying the linear standard electrode used in ECT in which needles with a diameter, D_{el}, of 0.7 mm are posed at inter-needle distance, d, of 2.5 mm. The length of external electrode has been studied using a Finite Element model.

FEM design

Model geometry is a parallelepiped (e.g. sizes 3×2×2.5 cm) with four cylinders that simulate the positions of the stainless steel needles, 0.7 mm diameter, represented in Fig 3. The parallelepiped describes a region made of a homogeneous material with a known resistivity (e.g. 60 Ωm). The external electrodes are made of stainless steel, whereas the cylinders, that represent voltage probes, are of the same material of the parallelepiped. In fact, it is supposed that they do not significantly perturb the current distribution since there are connected to the voltmeter that works as an open circuit. The external electrodes are supplied by imposing a constant voltage difference on the external electrodes. The correspondent electrical current has been evaluated by solving a static conduction problem. The following boundary value problem is solved on electric scalar potential, V [16]–[19] in order to evaluate the electric

field distribution:

$$\begin{aligned} \nabla \cdot \sigma \nabla V &= 0 && \text{inside the parallelepiped} \\ \frac{\partial V}{\partial n} &= 0 && \text{on external boundary} \end{aligned} \tag{3}$$

imposing a constant electric potential, V, on the two electrodes and a floating potential on the model boundary.
Given the electric field distribution in the tissue, the voltage difference between the internal electrodes has been evaluated. Using (2) the resistivity has been derived. Table 1 reports the results obtained varying the length L of the external electrode and the electrode diameter, D_el with an electrode distance d equal to 2.5 mm.. The length of the internal voltage electrode is 0.5 mm; anyway, this length is not mandatory since these electrodes measure the voltage in the area between the external electrodes without perturbing the electric field distribution.

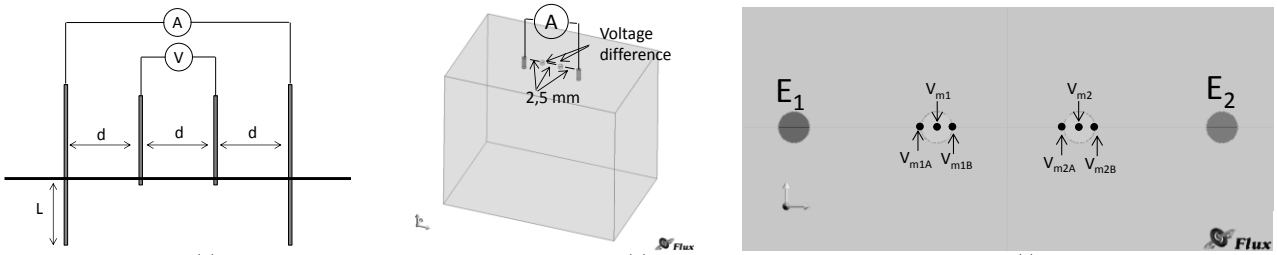

(a) (b) (c)

Fig 1 (a) schematic of the measurements set-up, (b) geometry of FEM model and (c) evaluation points for voltage measurements.

The voltage difference is measured between the center of electrodes, V_{m1} and V_{m2}, at a depth of 0.1 mm from the electrode surface. I_m is the applied current through the electrodes E_1 and E_2 in Fig. 1 (c). Finally, the resistivity ρ is evaluated with (2). Since the electric potential is not constant on the regions that describe the internal needles a resistivity interval, Δρ, has been evaluated considering the voltage variation on the electrode surface. For each electrode the voltage has been also evaluated in two pairs of points on needles surface, as shown in Fig 1(c). Considering the resistivity evaluated from these two voltage differences, V_{m1A} and V_{m2B}, ρ_+, or, V_{m1B} and V_{m2A}, ρ_-, in Fig 1(c), the interval of resistivity, Δρ, that is $(\rho_+ - \rho_-)/2$ has been computed.
From data in Table 1 it appears that the electrodes with a diameter of 0.7 mm and an inter-electrode distance d equals to 2.5 mm with an electrode length between 0.5 and 2 mm give a better evaluation of the actual resistivity that has been fixed equal to 60 Ωm (gray rows in Table 1). A lower electrode diameter underestimates the resistivity as well as longer electrodes.

Table 1 Results of FEM simulations

L [mm]	D_{el} [mm]	d [mm]	**V_{m1} [V]**	**V_{m2} [V]**	**I_m [A]**	**ρ [Ωm]**	**Δρ [Ωm]**
0.2	0.5	2.5	519.54	466.36	0.02	45.691	9.4
0.5	0.5	2.5	527.94	450.49	0.03	44.274	8.6
1.0	0.5	2.5	550.93	432.69	0.04	50.712	9.5
2.0	0.5	2.5	567.86	418.01	0.05	47.453	8.5
4.0	0.5	2.5	587.79	432.67	0.07	33.316	6.9
5.0	0.5	2.5	589.17	420.61	0.09	28.625	5.4
0.2	0.7	2.5	530.26	468.51	0.02	49.068	13.4
0.5	0.7	2.5	537.67	445.04	0.03	50.529	11.9
1.0	0.7	2.5	566.61	449.16	0.03	53.766	13.5
2.0	0.7	2.5	590.46	443.54	0.05	47.331	11.9
4.0	0.7	2.5	598.44	427.27	0.08	34.228	9.3
5.0	0.7	2.5	594.98	423.44	0.10	27.868	7.0

Prototype and validation
From FEM results some prototypes of resistivity sensors have been constructed (example in Fig. 2 (a)). Size data are summarized in Table 2.
The first validation of the measurement device has been provided by measuring the resistivity of NaCl solution at 0.9%. The resistivity values have been measured with the new device and using the electrical conductivity meter HI8883 by Hanna Instruments, calibrated at 20 °C using the standard solution 'Crison conductivity standard 9710' (14,13 mSm^{-1} @

25°C). The measured conductivity of the solution is 13.7 mSm^{-1} (resistivity 73 Ωm).

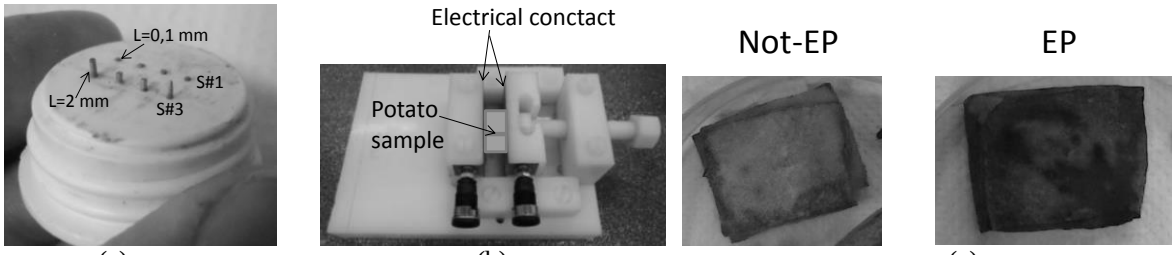

(a) (b) (c)

Fig 2 (a) Sensor prototype, (a) measurements set-up for potato sample and (c) not-electroporated (Not-EP) and electroporated (EP) potato tissue.

Table 2: evaluation of the electrical conductivity of a NaCl solution using the sensor.

	L [mm]	**D_{el} [mm]**	**d [mm]**	**V [V]**	**I [A]**	**d [mm]**	**σ [Sm^{-1}]**	**dev_st(σ)**	**ρ [Ωm]**
S#1	0.1	2.5	0.7	2.57	0.029	2.5	0.0072	0.0002	138.37
S#2	1.5	2.5	0.7	2.71	0.058	2.5	0.0139	0.0031	75.19
S#3	2	2.5	0.7	3.27	0.067	2.5	0.0134	0.0021	76.44
S#4	2.5	2.5	0.7	2.94	0.068	2.5	0.0150	0.0012	69.40

Results of these preliminary measurements are presented in Table 2. The sensors that give a more accurate evaluation of the resistivity are the ones with electrodes length of 1.5 or 2 mm. Longer electrodes, like L=2.5, overestimate the resistivity, whereas smaller electrodes underestimate this value. From these measurements it results that the probe S#2 and S#3 give an estimation of the resistivity close to the real one, as measured by electrical conductivity meter.

Potato tissue resistivity

The sensor S#2 has been tested to measure the resistivity of potato tissues. In this case the resistivity of potato tissue has been evaluated using the device in Fig. 2 (b). It is composed by two stainless steel contact with variable distance where the tissue sample can be positioned. A direct voltage has been applied by means of a DC voltage supply (GW GPR 1810H by Instek) and the corresponding electrical currents and applied voltages have been measured using a data logger (HP34970A, by HP). From the size of potato sample, measured using a vernier caliper, the resistivity, ρ, has been derived from the resistance value, R, measured at the contacts:

$$\rho = R\frac{A}{h} \tag{4}$$

where *A* is the area of the sample in contact with metal strip and *h* is the distance between metal contacts. From these measurements the range of the expected resistivity has been determined and measurement data are in Table 3.

Table 3 measurements of the potato resistivity using the device in Fig. 4. For resistivity and conductivity the sampling standard deviation is presented in bracket.

		V [V]	**I [A]**	**A [m2]**	**h [m]**	**d [mm]**	**ρ [Ωm]**	**σ [Sm^{-1}]**
Fig. 2 (b)		10.04	$1.80\cdot10^{-4}$	$9.2\cdot10^{-6}$	0.0155		33.11	0.030
Fig. 2 (b)		14.18	$2.63\cdot10^{-4}$	$9.2\cdot10^{-6}$	0.0155		32.00	0.031
Fig. 2 (b)		15.42	$2.48E\cdot10^{-4}$	$1.04\cdot10^{-5}$	0.0155		41.72	0.024
Fig. 2 (b)		15.16	$1.20\cdot10^{-4}$	$3.78\cdot10^{-6}$	0.0155		30.81	0.032
Fig. 2 (b)		15.18	$2.44\cdot10^{-4}$	$1.37\cdot10^{-5}$	0.0155		54.79	0.018
Fig. 2 (b)		10.47	$9.00\cdot10^{-5}$	$3.78\cdot10^{-6}$	0.0155		28.37	0.035
Fig. 2 (b)	**Sample A**	**10.75**	**$3.70\cdot10^{-4}$**	**$1.65\cdot10^{-5}$**	**0.016**		**30.02**	**0.033**
Fig. 2 (b)	**Sample A**	**10.68**	**$3.98\cdot10^{-4}$**	**$2.1\cdot10^{-5}$**	**0.016**		**35.22**	**0.028**
Average							**35.76 (±8.15)**	**0.029 (±0.005)**
S#3		2.3	$11.15\cdot10^{-4}$			2.5	32.40	0.031
S#3		2.08	$10.78\cdot10^{-4}$			2.5	30.31	0.033
S#3		2.1	$11.6\cdot10^{-4}$			2.5	28.44	0.035
S#3	**Sample A**	1.62	$8.05\cdot10^{-4}$			2.5	31.61	0.032
Average							**30.69 (±1.50)**	**0.033 (±0.001)**

Some measurements of resistivity have been carried out also with the sensor (S#3), with the same instrumentation described before. Results are reported in Table 3. It appears that the estimated resistivity (or conductivity) using the two methods are comparable. The data identified with 'Sample A' are derived by the same potato tuber.
Finally data in Table 4 report the resistivity of electropored and not-electropored potato tissue. The electroporation has been induced by placing a piece of potato tissue (with a thickness of approximately 1 cm) in the device shown in Fig. 2 (b) and applying a suitable constant voltage difference for few seconds with the DC power supply TDK-Lambda (GEN 1500 W). The electroporation occurrence is evaluated by observing the color of the sample after 24 h: if the tissue is dark the electroporation occurred [20]–[22]. An example of electroporated and not electroporated sample is in Fig. 2 (c). For all the samples, the resistivity has been evaluated before and after the application of electric currents and reported in Table 4. A difference in measured value of resistivity can be observed between electropored and not-electropored in all the samples. Difference in resistance values of not-electropored tissue can be due to water content and microscopic characteristic of tissue (e.g. root start).

Table 4 measurements of the potato resistivity using the device in Fig. 2(a) of electropored and not-electropored tissue (standard deviation in bracket).

	ρ [Ωm] – not-EP	**ρ [Ωm] - EP**	**Thickness [mm]**	**Applied voltage [V]**	**E [V/cm]**
sample 1	19.92 (± 3.39)	14.49 (± 1.03)	9.60	37.50	39.06
sample 2	21.64 (± 1.99)	12.46 (± 0.30)	9.20	42.00	45.65
sample 3	14.83 (± 3.21)	7.60 (± 0.41)	9.60	37.50	39.06
sample 4	18.83 (± 0.55)	11.02 (± 0.22)	9.40	37.50	39.89

Conclusion

The paper presents the design of a probe to measure resistivity of biological tissue. Experimental tests have been carried out to assess the measurements reliability by using a conductivity meter. Further measurements have been carried out on electroporated and not-electroporated potato tissue.

References

[1] L. M. Mir, (2001), *Bioelectrochemistry*, 53, 1–10.
[2] M. Marty, G. Sersa, J. R. Garbay, J. Gehl, C. G. Collins, M. Snoj, V. Billard, P. F. Geertsen, J. O. Larkin, D. Miklavcic, I. Pavlovic, S. M. Paulin-Kosir, M. Cemazar, N. Morsli, D. M. Soden, Z. Rudolf, C. Robert, G. C. O'Sullivan, L. M. Mir, (2006), *Eur. J. Cancer Suppl.*, 4, 3–13.
[3] L. Campana, S. Mocellin, M. Basso, O. Puccetti, G. De Salvo, V. Chiarion-Sileni, A. Vecchiato, L. Corti, C. Rossi, D. Nitti, (2009), *Ann. Surg. Oncol.*, 16, 191–199.
[4] L. Campana, G. Bianchi, S. Mocellin, S. Valpione, L. Campanacci, A. Brunello, D. Donati, E. Sieni, C. Rossi, (2014), *World J. Surg.* 813–822,.
[5] G. Sersa, D. Miklavcic, M. Cemazar, Z. Rudolf, G. Pucihar, M. Snoj, (2008), *Eur. J. Surg. Oncol.* 34, 232–240.
[6] M. Pavlin, N. Pavselj, e D. Miklavcic, (2002), *IEEE Trans. Biomed. Eng.*, 49. 605–612.
[7] R. Susil, D. Šemrov, D. Miklavčič, (1998), *Electromagn. Biol. Med.* 17, 391–399.
[8] J. Dermol, D. Miklavčič, (2014), *Bioelectrochemistry*, 100, 52–61.
[9] R. Scorretti, N. Burais, L. Nicolas, A. Nicolas, (2005), *IEEE Trans Magn.*, 41, 1992–1995.
[10] B. Kos, A. Zupanic, T. Kotnik, M. Snoj, G. Sersa, D. Miklavcic, (2010), *J. Membr. Biol.*, 236, 147–153.
[11] F. Wenner, (1916), *Bull. Bur. Stand.*, 12, 469.
[12] Report 81-1983 "IEEE Guide for Measuring Earth Resistivity, Ground Impedance, and Earth Surface Potentials of a Ground System Part 1: Normal Measurements"», 1983.
[13] Y. Wang, P. H. Schimpf, D. R. Haynor, Y. Kim, (1998), *IEEE Trans. Biomed. Eng.* 45, 877–884.
[14] S. Rush, J. A. Abildskov, R. Mcfee, (1963), *Circ. Res.*, 12, 40–50.
[15] H. C. Burger, J. B. van Milaan, (1943), *Acta Med. Scand.*, 114, 584–607.
[16] L. G. Campana, P. Di Barba, F. Dughiero, C. R. Rossi, E. Sieni, (2013), *IEEE Trans. Magn.* 49, 2141–2144.
[17] FLUX, «(CEDRAT): www.cedrat.com/software/flux/flux.html».[last visit July 2015]
[18] S. Corovic, I. Lackovic, P. Sustaric, T. Sustar, T. Rodic, e D. Miklavcic, (2013), *Biomed. Eng. OnLine*, 12, 16,
[19] P. Di Barba, A. Savini, S. Wiak, (2008) Field models in electricity and magnetism. [Dordrecht]: Springer.
[20] M. Castiello, F. Dughiero, F. Scandola, E. Sieni, L. G. Campana, C. R. Rossi, M. D. Mattei, A. Pellati, A. Ongaro,(2014), *Dielectr. Electr. Insul. IEEE Trans. On*, 21, 1424–1432.
[21] M. Hjouj e B. Rubinsky, (2010), *J. Membr. Biol.*, 236, 137–146.
[22] A. Ongaro, L. G. Campana, M. De Mattei, F. Dughiero, M. Forzan M., A. Pellati, C. R. Rossi, E. Sieni, (2015) *Technol. Cancer Res. Treat.*, doi: 10.1177/1533034615582350